

Kinetic and mechanistic studies of 1,3-bis(2-pyridylimino)isoindolate Pt(II) derivatives. Experimental and new computational approach†

Cite this: *Dalton Trans.*, 2014, **43**, 2549

Isaac M. Wekesa and Deogratius Jaganyi*

The rate of substitution of the chloride ligand by three bio-relevant nucleophiles, thiourea (**Tu**), *N,N*-dimethylthiourea (**Dmtu**) and *N,N,N,N*-tetramethylthiourea (**Tmtu**), in the complexes: 1,3-bis(2-pyridylimino)isoindoline platinum(II) chloride (**Pt2**), 1,3-bis(2-pyridylimino)benz(f)isoindoline platinum(II) chloride (**Pt3**) and 1,3-bis(1-isoquinolylimino)isoindoline platinum(II) complex (**Pt4**) was investigated under pseudo first-order conditions as a function of concentration and temperature using stopped-flow and UV-Visible spectrophotometry. Computational modeled data of bis(pyridylimino)3,4-pyrrolate platinum(II) chloride (**Pt1**) were incorporated in the study for comparison. The observed pseudo first-order rate constants for substitution reactions obey the rate law $k_{\text{obs}} = k_2[\text{Nu}]$. High negative activation entropies and second-order kinetics for the displacement reactions all support an associative mode of activation. The reactivity is dependent on stabilization of the LUMO energy and inversely proportional to the number of phenyl rings added irrespective of the site of attachment. The electron density on the ligand moiety plays a significant role in the substitution behavior of the platinum(II) complexes, as supported by DFT descriptors {electrophilicity index (ω) and chemical hardness (η)}.

Received 20th August 2013,
Accepted 18th November 2013

DOI: 10.1039/c3dt52272e

www.rsc.org/dalton

Introduction

Substitution reactions of square-planar Pt(II) complexes have attracted much attention from various investigators over the last two decades. The interest in this field continues uninterrupted as demonstrated by the large number of publications appearing annually.^{1,2–10} Some of these complexes are of special interest because of their application in homogeneous catalysis,^{11–13} as catalysts for C–H activation,^{14–17} and for anti-tumour treatment.^{18–26} The interaction of platinum based drugs with DNA is now widely accepted to be the mechanism responsible for their anticancer activity.^{27–33} Cisplatin [*cis*-diamminedichloroplatinum(II)] is one of the most active anti-tumour agents in clinical use.^{34–37} However, it has a narrow spectrum of activity and its clinical use is limited by undesirable side effects, including nephrotoxicity, ototoxicity, neurotoxicity, nausea, vomiting, and myelosuppression.^{27,29,38,39}

These drawbacks have provided an impetus for the development of novel and improved platinum antitumor drugs, with focus on the development of new derivatives that display improved therapeutic properties.

To design drugs with specific kinetic and thermodynamic properties, understanding the factors that control the reactivity of these complexes through a systematic investigation is important. To this effect many kinetic studies have been carried out on model Pt(II) complexes with terdentate ligands of the type (N[^]N[^]N[^]), (C[^]N[^]N[^]) and (N[^]C[^]N[^]).^{4,40–43} The studies have shown that when σ -donor groups (phenyl⁴³/methyl⁴¹/*t*-butyl^{9,41}) are attached or bonded *cis* to the core ligand, lower rates of substitution at the Pt(II) centers are observed due to their positive inductive donation of electron density to the metal center.⁴⁰ In contrast, when the σ -donating groups (phenyl) are attached to the *trans* position, this results in an increased lability owing to the well-known *trans*-labilizing effect.⁴³ It has also been shown that extended π -conjugation with pyridine as part of the aromatic ring enhances π -backbonding owing to a favourable overlap of the $d\pi$ -orbitals of the metal and the π^* -orbitals of ligands.^{4,42,44} Moreover, it emerged that the *cis*- π acceptor has a stronger influence on the reactivity of the metal centre than the *trans* π -acceptor whilst the π -acceptor effects of a conjugated system are multiplicative.^{4,40–42}

Against this backdrop, DFT calculations have been employed to give an insight into the electronic and steric

School of Chemistry and Physics, University of KwaZulu-Natal, Scottsville, 3209, Pietermaritzburg, South Africa. E-mail: jaganyi@ukzn.ac.za

† Electronic supplementary information (ESI) available: Selected mass and NMR spectra, wavelengths for kinetic measurements, observed pseudo-first-order rate constants, k_{obs} at different concentrations and temperatures, for **Pt2**, **Pt3** and **Pt4**. Concentration dependence plots for **Pt3** and **Pt4**. Eyring plots for **Pt3** and **Pt4**. UV/Visible kinetic overlay spectra of **Pt3** and **Tmtu** at 298.15 K. See DOI: 10.1039/c3dt52272e

properties of complexes; in addition, NBO charge on the metal center has been used effectively by Jaganyi *et al.*^{1,8,9,45} to explain the degree of electron deficiency in a given complex. Nonetheless, the challenge of NBO charge has always been the small magnitude of difference and sometimes inconsistency with reactivity.^{6,7,46} Inspired by the success of using global reactivity descriptors^{47,48} in predicting the chemical reactivity and addressing NBO charge inadequacies, chemical hardness (η), electronic chemical potential (μ) and electrophilicity index (ω) were incorporated in the study to unravel the intrinsic electronic properties of platinum(II) complexes. These reactivity descriptors have been reported to predict the biological activity/toxicity/properties of organic systems,^{49,50} synthetic chalcones,⁵¹ and several *cis*-platinum(II) complexes.⁵²

Accordingly, the kinetic properties of a complex can be tuned by structural modification of the π -conjugated ligand framework. This can be achieved by attaching donor and/or acceptor groups or extending the π -conjugation, particularly through benzannulation (addition of phenyl rings).⁵³ The intriguing aspect of extended π -conjugation is commonly assumed to destabilize the HOMOs which are about transfer of electrons from the ligand to the metal and stabilize the LUMOs by transfer of electrons from the metal centre to the ligand resulting in an increased lability. We take into account that increased π -conjugation narrows the HOMO–LUMO gap.⁵³ A perusal of the literature data shows limited mechanistic information on Pt(II) complexes bearing tridentate six-membered chelate ligands with methylene^{10,54} or amino spacer groups as part of the chelate ring. Based on this perspective we were compelled to expand the chelate ring size from conversional five-membered to six-membered chelates in an N[^]N[^]N[^] fashion with the amino group as part of the chelate ring.

We also sought to consolidate the effect of extended π -conjugation on the ligand core by successive addition of phenyl rings (benzannulation) in *trans* and *cis*-positions; hence, the substitution behaviour of platinum(II) complexes with 1,3-bis(2-pyridylimino)isoindoline ligands by three neutral bio-relevant nucleophiles (**Nu**) of different steric demands, namely thiourea (**Tu**), *N,N*-dimethylthiourea (**Dmtu**) and *N,N,N,N*-tetramethylthiourea (**Tmtu**), was studied. The structures of the investigated complexes **Pt2–Pt4** are shown in Scheme 1. DFT reactivity descriptors were incorporated in the study to broaden the interpretation of the kinetic data. **Pt1** is included for comparison purposes through DFT calculations.

Experimental section

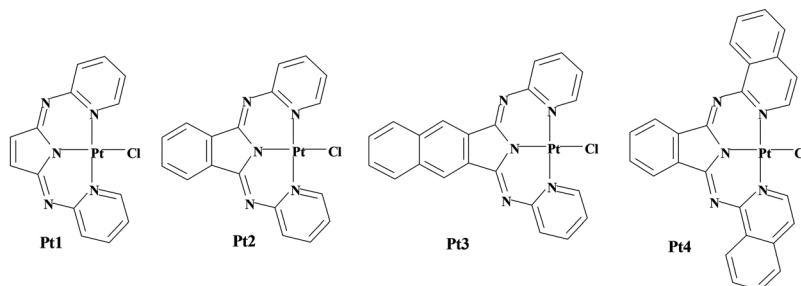
General procedures and chemicals

All synthetic work was performed under a dry and oxygen-free nitrogen atmosphere using standard Schlenk-ware techniques. Solvents were dried by standard methods and distilled prior to use. 1,2-Dicyanobenzene, 1-butanol, 1,3-diiminobenz(*f*)isoindoline, 2-aminopyridine, 1-aminoisoquinoline and triethylene amine (NEt₃), thiourea (**Tu**), 1,3-dimethyl-2-thiourea (**Dmtu**) and 1,1,3,3-tetramethyl-2-thiourea (**Tmtu**) were obtained from Aldrich and used without further purification. Anhydrous calcium chloride (CaCl₂) was obtained from Saarchem (South Africa) and used as supplied. The K₂PtCl₄ precursor for (COD)PtCl₂⁵⁵ was procured from STREM and used as received. The ligands 1,3-bis(2-pyridylimino)isoindole,⁵⁶ 1,3-bis(2-pyridylimino)benz(*f*)isoindoline,⁵⁷ 1,3-bis(1-isoquinolyimino)isoindole and platinum complexes were prepared according to published procedures.⁵³

Synthesis of ligands

1,3-Bis(2-pyridylimino)isoindoline(Z). A mixture of 1,2-dicyanobenzene (1.306 g, 10 mmol), 2-aminopyridine (1.98 g, 21 mmol), CaCl₂ (0.11 g, 1 mmol) and 20 mL 1-butanol was added to the reaction flask and refluxed under a nitrogen atmosphere for 48 hours. Upon cooling to ambient temperature, the green-yellow solid precipitate was formed, washed with water and finally purified by recrystallization with equal amounts of ethanol and water (1.98 g, 65.7%). ¹H NMR (400 MHz, CDCl₃, ppm) δ = 14.04 (s, N–H broad), 8.63 (m, 2H), 8.11 (m, 2H), 7.85–7.75 (m, 2H), 7.67 (m, 2H), 7.49 (d, 2H), 7.13 (m, 2H). ¹³C NMR (400 MHz, CDCl₃, ppm) δ = 160.6, 153.7, 147.7, 138.0, 135.7, 131.7, 123.2, 122.6, 120.1. TOF MS ES⁺, *m/z*: 300.1248 (M + 1)⁺.

1,3-Bis(2-pyridylimino)benz(*f*)isoindoline(Z). An oven dried reaction flask equipped with a magnet stir bar was filled with 1,3-diiminobenz(*f*)isoindoline (0.348 g, 1.78 mmol), 2-aminopyridine (0.336 g, 3.57 mmol), CaCl₂ (0.0195 mg, 0.178 mmol) and 20 mL 1-butanol, and then the resulting mixture was refluxed for 1 day. After cooling to room temperature, the resulting green-yellow precipitate was filtered off, washed with hexane, and the filtrate dried under vacuum. The crude product was purified by chromatography on a silica gel column using dichloromethane–acetone (100 : 1) as the eluent. The title green/yellow solid was collected as a second fraction



Scheme 1 Formulae of platinum(II) complexes investigated.

(0.135 g, 22%). ^1H NMR (400 MHz, CDCl_3 , ppm): δ = 14.60 (s N–H broad, 1H), 8.81 (s broad, 2H), 8.65 (dd, 2H), 8.1 (dd, 2H), 7.83 (td, 2H), 7.66 (dd, 4H), 7.20–7.16 (m, 2H). ^{13}C NMR (400 MHz, CDCl_3 , ppm) δ = 193.9, 165.2, 162.8, 157.0, 152.9, 137.9, 128.9, 124.1, 119.8, 115.7. TOF MS ES⁺, m/z : 350.1411 ($\text{M} + 1$)⁺.

1,3-Bis(1-isoquinolylimino)isoindoline(Z). A mixture of 1,2-dicyanobenzene (0.210 g, 1.15 mmol), 1-aminoisoquinoline (0.5 g, 3.45 mmol) and CaCl_2 (0.055 g, 0.5 mmol) in 20 mL 1-butanol was added to a reaction flask and refluxed under N_2 for 5 days. Upon cooling the reaction mixture to room temperature, the precipitate was formed. The precipitate was collected by filtration and washed with copious amounts of water under vacuum to give a golden yellow solid (0.470 g, 71.5%). *Anal. Calc. for* $\text{C}_{26}\text{H}_{18}\text{N}_5$; C: 78.19, H: 4.64, N: 17.54. *Found*; C: 78.57, H: 4.98, N: 17.19. ^1H NMR (400 MHz, CDCl_3 , ppm) δ = 9.05 (d, 2H), 8.54 (d, 2H), 8.23 (s, N–H broad), 7.82 (dd, 2H), 7.77–7.70 (m, 4H), 7.67 (t, 2H), 7.51 (dd, 2H). ^{13}C NMR (400 MHz, CDCl_3 , ppm) δ = 158.4, 137.7, 136.2, 131.8, 130.5, 127.0, 126.6, 126.2, 122.8, 118.2 TOF MS ES⁺, m/z : 400.1558 ($\text{M} + 1$)⁺.

Synthesis of the complexes

Dichloro[(1,2,5,6- η)-1,5-cyclooctadiene]platinum(II), (COD)PtCl₂. K_2PtCl_4 (2.5 g, 6 mmol) was dissolved in 40 mL H_2O and filtered. To the filtrate, 60 mL glacial acetic acid and 2.5 mL (20 mmol) of 1,5-cyclooctadiene were added. The mixture was refluxed at 90 °C for 1 hour. The solution turned from deep red to yellow with a light yellow precipitate. The volume was reduced to 30 mL and filtered. The precipitate formed was then washed with water, ethanol and ether and dried under vacuum. The product was used without further purification or characterization (1.56 g, 70%).

1,3-Bis(2-pyridylimino)isoindoline platinum(II) chloride, Pt2. Quantities of (COD)PtCl₂ (0.4 g 1.04 mmol) and 1,3-bis(2-pyridylimino)isoindoline (0.28 g 0.96 mmol) were suspended in 20 mL of methanol. After the addition of NEt_3 (143 μL , 1.04 mmol), the mixture was heated to 50 °C under a nitrogen atmosphere overnight. Upon cooling to room temperature, the precipitate formed. The crude platinum complex and $\text{NEt}_3\text{-HCl}$ were isolated by filtration and the ammonium salt removed by extraction with water. The orange product was further washed with water, ethanol, methanol and diethyl ether (0.438 g, 86%). *Anal. Calc. for* $\text{C}_{18}\text{H}_{12}\text{N}_5\text{PtCl}$; C: 40.83, H: 2.45, N: 13.23. *Found*; C: 40.68, H: 2.20, N: 13.64. ^1H NMR (500 MHz, d_6 -DMSO, ppm) δ = 10.16 (d, 2H), 8.20 (m, 2H), 8.09 (dd, 2H), 7.78 (dd, 2H), 7.69 (dd, 2H), 7.31 (m, 2H). TOF MS ES⁺, m/z : 529.0510 ($\text{M} + 1$)⁺.

1,3-Bis(2-pyridylimino)benz(f)isoindoline platinum(II) chloride, Pt3. A mixture of (COD)PtCl₂ (0.0654 g, 0.175 mmol), 1,3-bis(2-pyridylimino)benz(f)isoindoline (58 mg, 0.165 mmol), and NEt_3 (25 μL , 0.175 mmol) in 15 mL of methanol was refluxed for 12 h. After cooling to ambient temperature, the resulting red precipitate was filtered off, washed with water, a small amount of ethanol and Et_2O , and dried *in vacuo* (0.063 g, 62%). *Anal. Calc. for* $\text{C}_{22}\text{H}_{14}\text{N}_5\text{PtCl}$; C: 45.13, H: 2.42,

N: 12.20. *Found*; C: 44.95, H: 2.56, N: 11.99. TOF MS ES⁺, m/z : 543.0897 ($\text{M} - \text{Cl}$)⁺.

1,3-Bis(1-isoquinolylimino)isoindoline platinum(II) chloride, Pt4. A mixture of (COD)PtCl₂ (0.180 g, 0.481 mmol) and 1,3-bis(1-isoquinolylimino)isoindoline 0.192 g (0.481 mmol) was suspended in 20 mL of methanol. To this solution was added NEt_3 (66 μL , 0.481 mmol), and the mixture was heated to 50 °C under nitrogen for 24 h. Upon cooling the reaction mixture to room temperature, a precipitate formed. The precipitate was collected by filtration and washed with water, methanol, ethanol and Et_2O to give a dark purple solid (0.227 g, 75%). TOF MS ES⁺, m/z : 593.1053 ($\text{M} - \text{Cl}$)⁺. *Anal. Calc. for* $\text{C}_{18}\text{H}_{12}\text{N}_5\text{PtCl}$; C: 49.64, H: 2.54, N: 11.13. *Found*; C: 50.11, H: 2.26, N: 11.15.

Physical measurements and instrumentation

Either a Bruker Avance DPX 500 or DPX 400 NMR using a 5 mm BBOZ probe at 303 K was used to confirm the identity and purity of the ligands. Low resolution electron-spray ionization (ESI⁺) mass spectra of the samples were recorded on a TOF Micromass spectrometer operated in positive ion mode. Selected NMR and mass spectra are presented in Fig. S1–13, ESI.† Elementary compositions of the ligands and complexes were determined on a Carlo Erba Elemental Analyzer 1106 and a Thermo Scientific Flash 2000. UV-visible spectra and kinetic measurements of slow reactions were recorded on a Cary 100 Bio UV-visible spectrophotometer with a cell compartment thermostated by a Varian Peltier temperature controller having an accuracy of ± 0.05 °C. Kinetic measurements of fast reactions were monitored using an Applied Photophysics SX 20 stopped-flow reaction analyser coupled to an online data acquisition system. The temperature of the instrument was controlled to within ± 0.1 °C.

Kinetic measurements

The kinetic substitution of the coordinated chloride was followed spectrophotometrically by monitoring the change in absorbance at suitable wavelengths as a function of time using a Cary 100 Bio UV-visible spectrophotometer. The working wavelengths were pre-determined by recording spectra of the reaction mixture over the wavelength range 200–650 nm. All kinetic experiments were performed under pseudo-first order conditions, for which the concentration of the nucleophile was always in at least 10-fold excess. All substitution reactions were studied in 0.1 M NaClO_4 ethanolic solutions. The NaClO_4 was used because perchlorate ions do not coordinate to the Pt(II) center;⁵⁸ in addition, 10 mM LiCl was added to suppress any possibility of spontaneous solvolytic reactions. The reactions were initiated by mixing solutions of Pt4 and nucleophiles of equal volumes in a thermally equilibrated UV-Visible suprasil tandem cuvette. Subsequently, substitution reactions involving Pt2 and Pt3 were monitored directly on the Stopped-Flow instrument and followed for at least eight half-lives. The temperature dependence reactions were studied in the range of 20 °C to 40 °C with 5 °C intervals. All kinetic runs could be fitted to a non-linear single-exponential decay function. The

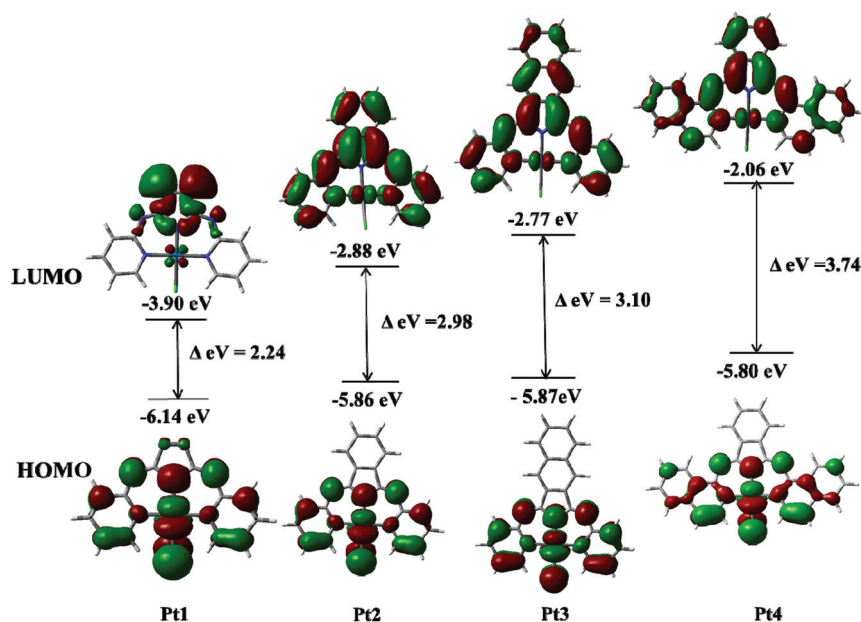


Fig. 1 DFT calculated structures showing frontier orbital mappings and respective energies for isoindoline complexes.

observed pseudo-first-order rate constant, k_{obs} , was calculated as the average value of 5–10 independent kinetic runs. The second-order rate constant, k_2 , for the reaction of each metal complex with a particular nucleophile was obtained from the slope of a linear regression of a plot of observed rate constant, k_{obs} , versus the nucleophile concentration using Origin 7.5® software.⁵⁹ A summary of the observed pseudo-first-order rate constant, k_{obs} , at different concentrations and temperatures is reported in Tables S1–7, ESI.†

Computational details

In order to gain an in-depth understanding of the structural and electronic differences that exist in the complexes under study, computational calculations were performed. Structures were optimized by means of density functional theory (DFT) using the hybrid Becke's three-parameter exchange functional and the correlation functional from Lee, Yang and Parr (B3LYP)^{60–62} This method is suitable for the calculations of systems containing heavy atoms⁶³ as in this study (Pt atoms). Furthermore, DFT calculations in systems involving transition metals have proved to be in better agreement with experimental data than those obtained from Hartree–Fock (HF) calculations.⁶⁴ In the present case, the LANL2DZ basis set was employed as it is known to provide reliable results in systems involving transition metal atoms.^{63,65–68} The singlet states were used due to the low electronic spin of Pt(II) complexes. In addition, frequency calculations at the same level of theory were performed to identify the stationary points as minima (zero imaginary frequencies) or transition states (negative imaginary frequency). The frontier molecular orbitals of these complexes were generated in Gauss view 5.0 using the same level of theory. The Gaussian09 suite of programs was used for all DFT computations.⁶⁹ The calculated optimized structures

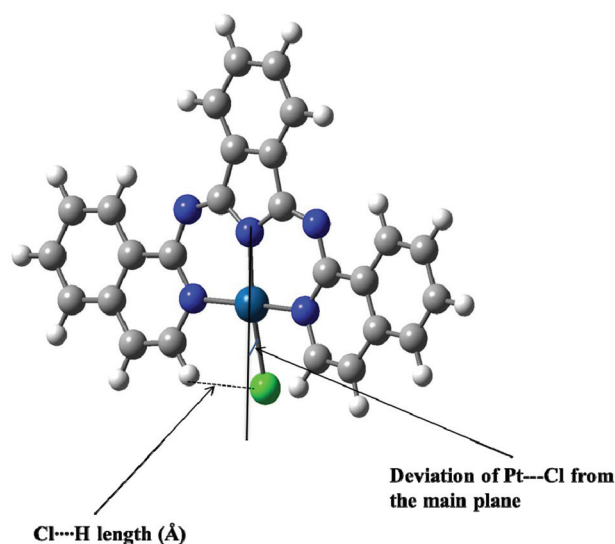


Fig. 2 DFT optimized structure of Pt4 representing the angle of deviation from the coordination plane and chlorine *ipso* hydrogen lengths.

and key geometrical data are summarized in Fig. 1 and 2 and Table 1, respectively.

Results and discussion

Theoretical background

The forming and breaking process of covalent bonds during the interaction of electron-rich and electron-poor centres,^{70–72} described as nucleophile–electrophile interaction, is one of the fundamental processes in chemistry, which is the rationale behind the mechanism of reacting species. Due to the success

Table 1 Summary of DFT calculated data for investigated complexes

Property	Pt1	Pt2	Pt3	Pt4
Bond lengths (Å)				
<i>Trans</i> N–Pt	1.997	2.002	2.007	1.995
<i>Cis</i> N–Pt	2.080	2.084	2.104	2.082
Pt–Cl	2.475	2.473	2.476	2.473
Cl...H	2.28	2.29	2.20	2.30
Angles (°)				
Bite	173.72	173.62	179.91	172.89
Dihedral	19.93	20.00	–	22.78
<i>Trans</i> N–Pt–Cl	169.75	169.53	180.00	168.00
Deviation of Pt–Cl From the main axis	10.25	10.47	0.09	12.00
Energy gap (eV)				
LUMO energy (eV)	–3.90	–2.88	–2.77	–2.06
HOMO energy (eV)	–6.14	–5.86	–5.87	–5.80
$\Delta E_{\text{LUMO-HOMO}}$	2.24	2.98	3.10	3.74
NBO charges Pt ²⁺	0.527	0.5222	0.527	0.529
Dipole moment (<i>D</i>)	2.81	3.07	3.54	4.35
Electronic chemical potential (μ)	–5.02	–4.37	–4.32	–3.93
Electrophilicity index (ω)	8.94	6.41	6.02	4.13
Chemical hardness (η)	2.24	2.98	3.10	3.74

of DFT-based descriptors in predicting the reactivity of organic and inorganic compounds,^{73,74} descriptors such as chemical hardness (η), ionization potential (*I*), electron affinity (*A*), electronegativity (χ), chemical potential (μ) and electrophilicity index (ω) were incorporated in the current study to aid the understanding of experimental data. Chemical hardness is associated with the stability and reactivity of a chemical system. In a complex, it measures the resistance to change in the electron distribution in a collection of nuclei and electrons.^{47,75}

On the basis of frontier molecular orbitals, chemical hardness corresponds to the HOMO–LUMO gap as expressed in eqn (1).

$$\eta = I - A = E_{\text{LUMO}} - E_{\text{HOMO}} \quad (1)$$

where *I* and *A* are absolute values of HOMO and LUMO energies respectively. The larger the HOMO–LUMO gap, the harder and less reactive the complex.⁷⁶ Moreover, a system with higher values of electron affinity (*A*) and ionization potential (*I*) has a preference for accepting electrons.⁷⁷ Table 1 contains the computed values of chemical hardness; the results indicate that **Pt1** is soft and has a high propensity for accepting electrons; hence, one will expect it to be more reactive than **Pt2**, **Pt3** and **Pt4**.

Electronic chemical potential is defined as the negative of electronegativity of a chemical species⁷⁸ and is determined using eqn (2). Physically, it describes the escaping tendency of electrons from an equilibrium system.⁷⁶ The higher the electronic chemical potential, the more reactive the chemical species, though the trend is not in line with experimental data; the apparent violation can be ascribed to improper chemical potential.⁴⁷

$$\mu = -\chi = -\left[\frac{I + A}{2}\right] \quad (2)$$

Consequently, a measure of the electrophilicity index depends on chemical potential, chemical hardness and electronegativity as shown in eqn (3).

$$\omega = \frac{\mu^2}{2\eta} = \frac{(-\chi)^2}{2\eta} \quad (3)$$

The electrophilicity index measures the propensity or the capacity of a complex to accept electrons.⁴⁸ The index determines the stabilization in energy when the system acquires an additional electronic charge from the environment. The electrophilicity indices **Pt1**(8.94), **Pt2**(6.41), **Pt3**(6.02) and **Pt4**(4.13) in Table 1 show that **Pt4** is less electrophilic; therefore, the expectation is that it should be less reactive than **Pt1**, **Pt2** and **Pt3**, which is in accord with the observed rate constants. The electrophilicity index should not be confused with the NBO charge. The NBO charge denotes the individual atomic charge, whereas the electrophilicity index designates the resulting charge of the entire complex. Thus, the electrophilicity index is superior to the NBO charge in predicting the reactivity of metal complexes. Further details are presented in the Discussion section (*vide infra*).

Results

Substitution of coordinated chloride (reaction (1)) from the Pt(II) complexes (Scheme 1) by three different nucleophiles (**Nu**), *i.e.*, thiourea (**Tu**), 1,3-dimethyl-2-thiourea (**Dmtu**) and 1,1,3,3-tetramethyl-2-thiourea (**Tmtu**), was investigated under pseudo-first-order conditions using conventional UV-Visible spectrophotometry and the stopped-flow technique. A typical stopped-flow kinetic trace at 504 nm recorded by mixing ethanol solutions of **Pt2** and 50 times the concentration of **Dmtu** at an ionic strength of 0.1 M (NaClO₄) is shown in Fig. 3.

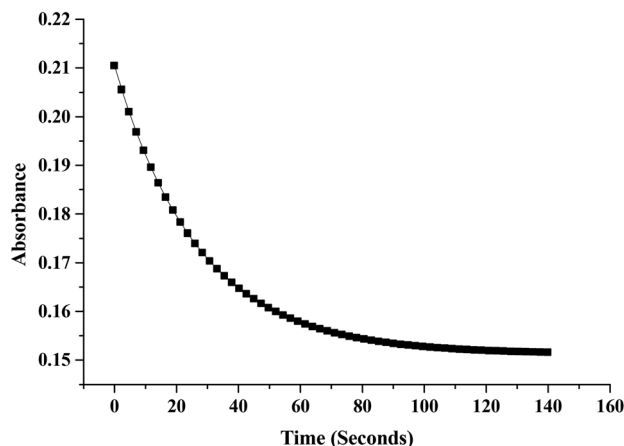
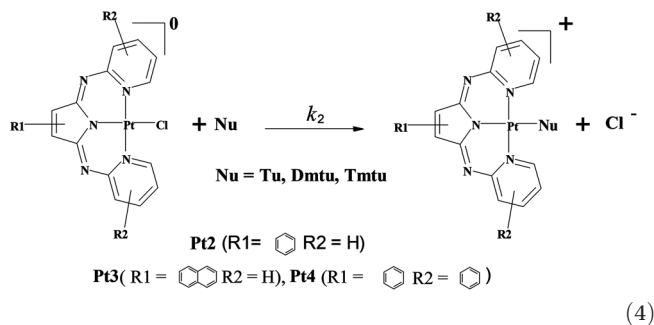


Fig. 3 Stopped-Flow kinetic trace of **Pt2** and **Dmtu** at 298 K.



The pseudo-first-order rate constant, k_{obs} , calculated from the kinetic traces, was plotted against the concentration of the incoming nucleophiles. Straight lines with zero intercepts were obtained for each of the entering nucleophiles, suggesting that the mechanism of the substitution can be represented by reaction (4) and the corresponding rate law given by eqn (5), indicating that a reverse or solvolytic pathway was absent or insignificant.

$$k_{\text{obs}} = k_2[\text{Nu}] \quad (5)$$

Representative plots are shown in Fig. 4 for **Pt2** (see also Fig. S14–15 for similar plots for **Pt3** and **Pt4**, ESI).[†] In all cases the reactions showed a first-order dependence on the concentration of the incoming nucleophile. The values of the second-order rate constant k_2 , which results from the direct attack of the nucleophile as shown in reaction (4), were obtained from the slopes of these plots at 25 °C and are summarized in Table 2. The temperature dependence of k_2 was studied over the range of 20 to 40 °C at intervals of 5 °C to determine the mode of mechanism of platinum(II) complexes. The activation parameters, ΔH^\ddagger and ΔS^\ddagger , were calculated using the Eyring equation.⁷⁹ The temperature dependence plots and activation data are represented in Fig. 5 and Table 2, respectively (see also Fig. S16–17 for **Pt3** and **Pt4**, ESI).[†]

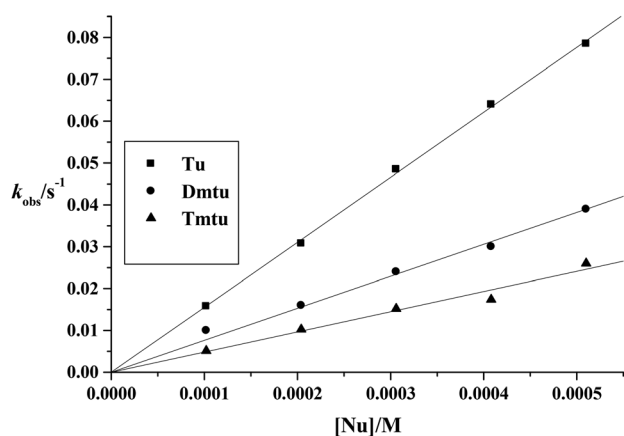


Fig. 4 Dependence of the pseudo-first-order rate constant (k_{obs}) on the concentration of thiourea nucleophiles for chloride substitution on **Pt2** in ethanol, $l = 0.1 \text{ M (NaClO}_4\text{)}$, $T = 298 \text{ K}$.

Table 2 Summary of rate constants and activation parameters for the substitution of chloride by **Tu**, **Dmtu** and **Tmtu** in ethanol, $l = 0.1 \text{ M (NaClO}_4\text{)}$

Complex	Nucleophile	$k_2/\text{M}^{-1} \text{ s}^{-1}$	$\Delta H^\ddagger/\text{kJ mol}^{-1}$	$\Delta S^\ddagger/\text{J K}^{-1} \text{ mol}^{-1}$
Pt2	Tu	155.3 ± 1.4	20 ± 1	-202 ± 4
	Dmtu	76.4 ± 1.7	60 ± 4	-70 ± 13
	Tmtu	48.2 ± 1.8	22 ± 1	-195 ± 4
Pt3	Tu	30.10 ± 0.50	41 ± 4	-125 ± 14
	Dmtu	6.22 ± 0.06	52 ± 4	-103 ± 15
	Tmtu	0.20 ± 0.10	36 ± 3	-187 ± 11
Pt4	Tu	0.98 ± 0.11	34 ± 1	-201 ± 4
	Dmtu	0.63 ± 0.20	43 ± 2	-175 ± 5
	Tmtu	0.55 ± 0.01	37 ± 2	-199 ± 9

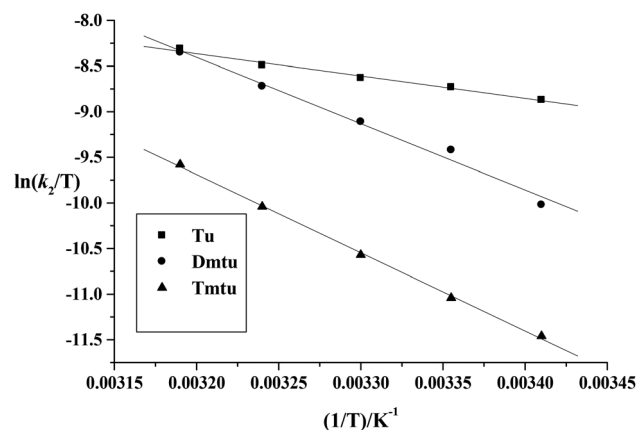


Fig. 5 Eyring plots of **Pt2** with thiourea nucleophiles at different temperatures.

Discussion

In the current study, phenyl rings were attached to the core ligand at different sites to bring about varying degrees of extended π -conjugation. To accomplish this, three complexes were tailor synthesized and their substitution behavior studied with bio-relevant thiourea nucleophiles. The thiourea nucleophiles were chosen because of their different nucleophilicity, steric hindrance, binding properties, and biological relevance. Thiourea is a very useful nucleophile since it combines the ligands of thiolates (σ -donor) and thioethers (σ -donor and π -acceptor).^{80–82} In addition, it is used as a protecting agent to minimize nephrotoxicity following cisplatin treatment.²⁹ A cursory look by a mechanistic erudite at the structures will predict high reactivities for **Pt3** and **Pt4** based on their levels of extended π -conjugation^{4,42,61} comparative to **Pt2**. However, the experimental data reveal the opposite, whereby k_2 values follow the order **Pt2** ($155.3 \text{ M}^{-1} \text{ s}^{-1}$) > **Pt3** ($30.1 \text{ M}^{-1} \text{ s}^{-1}$) > **Pt4** ($0.98 \text{ M}^{-1} \text{ s}^{-1}$) in Table 2, with **Tu** as an entering nucleophile. The observed reactivity is fundamentally related to their inherent electronic and steric properties.

The coordination geometry of the complexes is square planar with virtually *cis*-N–Pt–Cl and *trans*-N–Pt–*cis*-N approximately 90.0° with *trans*-N–Pt–Cl angles (**Pt1**, 169.75), (**Pt2**,

169.53°), (**Pt3**, 179.91°) and (**Pt4**, 168.00°) as shown in Table 1. The steric congestion emanating from chlorine and *ipso*-hydrogens {Cl...H \approx 2.28 Å (**Pt1**), 2.28 Å (**Pt2**), 2.20 Å (**Pt3**), 2.30 Å (**Pt4**)} is coupled with the Pt–Cl fragment warping away 10.25° (**Pt1**), 10.47° (**Pt2**), 0.09° (**Pt3**), and 12° (**Pt4**) from the coordination plane as illustrated in Fig. 2. This deviation introduces steric hindrances to the incoming nucleophile. It is worth noting the insignificant angle of deviation from planarity of **Pt3** which can be attributed to the strong *trans*- σ/π donating naphthalene moiety that levels off the bending away of Pt–Cl fragment resulting in a planar symmetric C_{2v} structure. Nonetheless, this feature contrasts with the observed low reactivity of **Pt3**, an indication that the steric hindrance plays a minor role in these reactivities. Similarly, the more perfect square-planar structures of the six-membered chelate complexes under study confer stronger field strength from the ligand owing to minimal ring strain due to a more optimal bite angle at the metal ion close to 180°^{53,65,83} as shown in Table 1, encumbers reactivity compared to five-membered chelates.^{1,4,7,8,41,43,45}

The mappings of frontier orbitals (Fig. 1) compare satisfactorily with those determined previously by the Hanson⁵³ and Wen⁶⁵ research groups. The LUMOs are centred entirely on whole complexes with the exception of **Pt1** which is aligned on the pendant pyrrolate fragment and low energy 5d_{xz} orbital of the platinum atom whilst the HOMOs are predominantly concentrated on the [(pyridylimino)3,4-pyrrolate]PtCl portion, and thus the HOMO energies appear to be dictated by this moiety. This is consistent with the view that the isoindoline moieties are good electron donors. The HOMOs consist of contributions from the respective p and d-orbitals of the chloride and platinum atoms, as well as from the π -system of the pyridyl and imino-pyrrolate portions of the ligand. There is an insignificant change in the appearance of the HOMO density with an increase in benzannulation resulting in invariant HOMO energies that are manifested by the electronic isolation from the site of benzannulation⁵³ (Fig. 1). The LUMOs are localized primarily on the π -system of the ligand with only a small contribution from the d-orbital on the Pt atom.

As depicted by the frontier molecular orbitals in Fig. 1, the LUMOs of the complexes are significantly contributed by the lowest π^* -{carbon (phenylene or naphthylene) or N-containing moiety} orbitals whilst the HOMOs are mainly contributed by the highest π -N-containing moiety. The molecular calculations show that the HOMOs correspond to the out-of-phase combination between the carbon moiety and the N-containing moiety, whilst the LUMOs are an in-phase combination of the π^* -orbitals of the two moieties.⁶⁵ The π -orbitals of the N-containing moiety and the carbon moiety differ significantly in their orbital energies so that the orbital interaction between them is less significant and the HOMOs are N-containing moiety based. As a consequence, the HOMOs have similar orbital energy; in contrast, the LUMOs arise from π^* -orbital interaction between the carbon moiety and the N-containing one, in which the π^* -orbitals of the two moieties have similar orbital energies. As a result, the orbital interaction is more

significant for **Pt1**, so as to give a lower energy of LUMO, hence leading to a smaller HOMO–LUMO gap as shown in Fig. 1. In more conjugated systems, the energy match between the π^* -orbitals of carbon and N-containing moieties worsens with each successive addition of phenyl rings, thus resulting in high LUMO energies for the **Pt2**, **Pt3** and **Pt4** complexes.

In addition, analysis of the LUMO energies depict an unusually high value for **Pt4** (–2.06 eV) in relation to **Pt1** (–3.90 eV), **Pt2** (–2.88 eV) and **Pt3** (–2.77 eV), which makes it the poorest π -acceptor, leading to a destabilized transition state which is expected to result in more dampening of the general reactivity of **Pt4** compared to the others. It is also noted that the LUMO energies increase proportionately with the increase in the size of the π -surface but inversely with the observed reactivity of the complexes. Preceding studies have associated this phenomenon with molecular distortions (tetra-cyano-*p*-quinodimethane),⁸⁴ an increase in total antibonding character of the orbitals (in indoanilines and anhydrides)^{85,86} or an increased localization of the π^* orbital on the complexes,⁸⁷ which is evident with the LUMO mappings in these studies. A direct relationship is noticed between the reactivity trend and HOMO–LUMO energy gaps as well as the electrophilicity indices (see Table 1). In contrast, NBO charges at the Pt(II) center remain unchanged despite the change in the size of the π -surface, suggesting that the metal centre is not experiencing any change in electron density even though the electrophilicity index which measures the degree of electron deficiency in the entire complex⁴⁸ shows a clear trend of decreasing as the π -conjugation increases. The unchanging NBO charge (which represents the charge on the platinum atom) is due to the presence of electronegative pyridylimino arm-N atoms which shield the platinum atom from electronic influence around it, as the phenyl rings get added to it. The apparent increase in dipole moments with subsequent addition of phenyl rings is expected given that the parameter correlates to the inductive⁸⁸ negative charge in the complex.

One can therefore conclude that it is not the change in the charge on the metal that influences the reactivity but the general increase in the negative charge on the ligand moiety which controls the reactivity. This is supported by the DFT calculation in determining the electrophilicity indices of the complexes. This increase in electron density retards the reaction by repelling the incoming nucleophile. Comparing **Pt2** and **Pt3**, one would have expected **Pt3** to be more reactive because of the additional pendant phenyl ring which customarily has a *trans*-labilizing effect, but the opposite is observed. As already explained, the resulting electron density that build up around the complexes in going from **Pt1** to **Pt4** corroborates with the calculated electrophilicity index as a function of the HOMO–LUMO gap (Table 1), which suggests a reduction in π -back donation. As a consequence, the HOMOs are stabilized and LUMOs are destabilized, causing an observed decrease in reactivity from **Pt2** to **Pt4**. Therefore, electrophilicity values confirm the σ/π -donating dominance over the π -backbonding.

A recent examination of electrochemical properties of the complexes by Wen *et al.*⁶⁵ and Hanson *et al.*⁵³ revealed that reduction peaks shifted to more negative values with each successive addition of phenyl rings (benzannulation), owing to molecular distortions of the fused phenyl rings rather than the electronic effect of increasing π -delocalization.^{89,90} The trend is counter to the common intuitive expectation that the species with the larger π -orbital system provide a greater stabilization to the negative charge.⁹¹ The more negative reduction potentials⁵³ for **Pt3** and **Pt4** validate the σ -donation dominance of quinoline^{1,45} and naphthalene moieties in **Pt4** and **Pt3**, respectively. The calculated electrophilicity indices support this notion.

The substitution of chloride by the nucleophiles **Tu**, **Dmtu** and **Tmtu** decreases according to the increasing steric hindrance of the nucleophiles for all the complexes, with the most sterically hindered **Tmtu** reacting significantly slower. The activation enthalpies (ΔH^\ddagger) are positive while the activation entropies (ΔS^\ddagger) are large and negative. The sensitivity of the second-order rate constants to the thiourea nucleophiles and the significantly negative intrinsic entropies of activation (ΔS^\ddagger) values are in line with the associative substitution mechanism, well known for d^8 square-planar metal complexes.^{92,93}

Conclusion

In this study, we have shown that the reactivity of Pt(II) complexes with a common bis(pyridylimino)3,4-pyrrolic ligand backbone can be systematically tuned by successive addition of phenyl rings (benzannulation) on the ligand framework. The results show an unusual retardation in reactivity with an increase in the expanded π -surface. This uncharacteristic behavior is linked to LUMO destabilization, which emanates from molecular distortions, shifts in total antibonding character or increased localization of the π^* orbitals. As exemplified by DFT calculations, the LUMO energy increases from **Pt1** to **Pt4**; thus, it is energetically unfavorable to add electrons to a high-lying LUMO, which impedes the π -electron acceptability. Moreover, the retarded lability in **Pt3** and **Pt4** is caused by the presence of poor π -acceptors and good π/σ -donors fragments, naphthalene in the case of **Pt3** and quinoline for **Pt4**. The common electronegative pyridimino arm-N within the chelate ring shields the platinum atom (unchanging NBO charge) from the electronic influence as the phenyl rings are added. The resulting electron density on the ligand motif plays a vital role in controlling reactivity as exhibited by DFT descriptors {electrophilicity index (ω) and chemical hardness (η)}. DFT descriptors provided a comprehensive approach for understanding the electronic properties of the studied complexes. The second-order kinetics and the dependence of the rate on the nature of the incoming group confirm the bimolecular character of the transition state since the data fit a reaction coordinate characteristic of a bond-making process, thus indicating an associative mechanism.

Acknowledgements

The authors are indebted to the University of KwaZulu-Natal and the National Research Foundation (NRF, Pretoria) South Africa for financial support.

References

- 1 A. Shaira, D. Reddy and D. Jaganyi, *Dalton Trans.*, 2013, **42**, 8426–8436.
- 2 P. O. Ongoma and D. Jaganyi, *Dalton Trans.*, 2013, **42**, 2724–2734.
- 3 A. Mijatović, J. Bogojeski, B. Petrović and Ž. D. Bugarčić, *Inorg. Chim. Acta*, 2012, **383**, 300–304.
- 4 A. Hofmann, D. Jaganyi, O. Q. Munro, G. Liehr and R. van Eldik, *Inorg. Chem.*, 2003, **42**, 1688–1700.
- 5 J. Bogojeski, Ž. D. Bugarčić, R. Puchta and R. van Eldik, *Eur. J. Inorg. Chem.*, 2010, **2010**, 5439–5445.
- 6 A. Mambanda and D. Jaganyi, *Dalton Trans.*, 2012, **41**, 908–920.
- 7 A. Mambanda and D. Jaganyi, *Dalton Trans.*, 2011, **40**, 79–91.
- 8 D. Reddy, K. J. Akerman, M. P. Akerman and D. Jaganyi, *Transition Met. Chem.*, 2011, **36**, 593–602.
- 9 D. Reddy and D. Jaganyi, *Dalton Trans.*, 2008, 6724–6731.
- 10 B. Petrović, Z. i. D. Bugarčić, A. Dees, I. Ivanović-Burmazović, F. W. Heinemann, R. Puchta, S. N. Steinmann, C. Corminboeuf and R. Van Eldik, *Inorg. Chem.*, 2012, **51**, 1516–1529.
- 11 S. Haneda, C. Ueba, K. Eda and M. Hayashi, *Adv. Synth. Catal.*, 2007, **349**, 833–835.
- 12 J. Durand, S. Gladiali, G. Erre, E. Zangrando and B. Milani, *Organometallics*, 2007, **26**, 810–818.
- 13 U. Fekl and K. I. Goldberg, *Adv. Inorg. Chem.*, 2003, **54**, 259–320.
- 14 L.-C. Liang, J.-M. Lin and W.-Y. Lee, *Chem. Commun.*, 2005, 2462–2464.
- 15 H. A. Zhong, J. A. Labinger and J. E. Bercaw, *J. Am. Chem. Soc.*, 2002, **124**, 1378–1399.
- 16 T. G. Driver, T. J. Williams, J. A. Labinger and J. E. Bercaw, *Organometallics*, 2007, **26**, 294–301.
- 17 L. Johansson, M. Tilset, J. A. Labinger and J. E. Bercaw, *J. Am. Chem. Soc.*, 2000, **122**, 10846–10855.
- 18 D. Leubwohl and R. Canetta, *Eur. J. Cancer*, 1998, **34**, 1522–1534.
- 19 Y. Kidani, M. Noji and T. Tashiro, *Gann = Gan*, 1980, **71**, 637.
- 20 A. Ghezzi, M. Aceto, C. Cassino, E. Gabano and D. Osella, *J. Inorg. Biochem.*, 2004, **98**, 73–78.
- 21 M. Jakupec, M. Galanski and B. Keppler, in *Reviews of physiology, biochemistry and pharmacology*, Springer, Editon edn, 2003, pp. 1–53.
- 22 K. Becker, C. Herold-Mende, J. J. Park, G. Lowe and R. H. Schirmer, *J. Med. Chem.*, 2001, **44**, 2784–2792.

- 23 P. C. Bruijninx and P. J. Sadler, *Curr. Opin. Chem. Biol.*, 2008, **12**, 197–206.
- 24 D. Wang and S. J. Lippard, *Nat. Rev. Drug Discovery*, 2005, **4**, 307–320.
- 25 H. Zorbas and B. K. Keppler, *ChemBioChem*, 2005, **6**, 1157–1166.
- 26 L. Kelland, *Nat. Rev. Cancer*, 2007, **7**, 573–584.
- 27 E. Wong and C. M. Giandomenico, *Chem. Rev.*, 1999, **99**, 2451–2466.
- 28 N. J. Wheate and J. G. Collins, *Coord. Chem. Rev.*, 2003, **241**, 133–145.
- 29 J. Reedijk, *Chem. Rev.*, 1999, **99**, 2499–2510.
- 30 E. R. Jamieson and S. J. Lippard, *Chem. Rev.*, 1999, **99**, 2467–2498.
- 31 A. Eastman, *Biochemistry*, 1986, **25**, 3912–3915.
- 32 S. E. Sherman and S. J. Lippard, *Chem. Rev.*, 1987, **87**, 1153–1181.
- 33 V. Brabec and J. Kasparkova, *Drug Resist. Updat.*, 2005, **8**, 131–146.
- 34 A. A. El-Sherif and M. M. Shoukry, *Inorg. Chim. Acta*, 2007, **360**, 473–487.
- 35 M. A. Barry, C. A. Behnke and A. Eastman, *Biochem. Pharmacol.*, 1990, **40**, 2353–2362.
- 36 B. Desoize and C. Madoulet, *Crit. Rev. Oncol./Hematol.*, 2002, **42**, 317–325.
- 37 G. V. Scagliotti, P. Parikh, J. von Pawel, B. Biesma, J. Vansteenkiste, C. Manegold, P. Serwatowski, U. Gatzemeier, R. Digumarti and M. Zukin, *J. Clin. Oncol.*, 2008, **26**, 3543–3551.
- 38 J. Lokich, *Cancer Invest.*, 2001, **19**, 756–760.
- 39 S. Shibata, A. Ochi and K. Mori, *Neurol. Med. Chir.*, 1990, **30**, 242.
- 40 D. Jaganyi, D. Reddy, J. Gertenbach, A. Hofmann and R. van Eldik, *Dalton Trans.*, 2004, 299–304.
- 41 D. Jaganyi, K. L. D. Boer, J. Gertenbach and J. Perils, *Int. J. Chem. Kinet.*, 2008, **40**, 808–818.
- 42 D. Jaganyi, A. Hofmann and R. van Eldik, *Angew. Chem., Int. Ed.*, 2001, **40**, 1680–1683.
- 43 A. Hofmann, L. Dahlenburg and R. van Eldik, *Inorg. Chem.*, 2003, **42**, 6528–6538.
- 44 M. Schmülling, D. M. Grove, G. van Koten, R. van Eldik, N. Veldman and A. Spek, *Organometallics*, 1996, **15**, 1384–1391.
- 45 P. Ongoma and D. Jaganyi, *Dalton Trans.*, 2012, **41**, 10724–10730.
- 46 P. O. Ongoma and D. Jaganyi, *Int. J. Chem. Kinet.*, 2013, **45**, 676–691.
- 47 C. A. Mebi, *J. Chem. Sci.*, 2011, **123**, 727–731.
- 48 R. G. Parr, L. v. Szentpály and S. Liu, *J. Am. Chem. Soc.*, 1999, **121**, 1922–1924.
- 49 J. Padmanabhan, R. Parthasarathi, V. Subramanian and P. Chattaraj, *Bioorg. Med. Chem.*, 2006, **14**, 1021–1028.
- 50 J. Padmanabhan, R. Parthasarathi, V. Subramanian and P. Chattaraj, *Chem. Res. Toxicol.*, 2006, **19**, 356–364.
- 51 C. Echeverria, J. F. Santibañez, O. Donoso-Tauda, C. A. Escobar and R. Ramirez-Tagle, *Int. J. Mol. Sci.*, 2009, **10**, 221–231.
- 52 P. Sarmah and R. C. DeKa, *J. Comput.-Aided Mol. Des.*, 2009, **23**, 343–354.
- 53 K. Hanson, L. Roskop, P. I. Djurovich, F. Zahariev, M. S. Gordon and M. E. Thompson, *J. Am. Chem. Soc.*, 2010, **132**, 16247–16255.
- 54 R. Romeo, M. R. Plutino, L. Monsù Scolaro, S. Stoccoro and G. Minghetti, *Inorg. Chem.*, 2000, **39**, 4749–4755.
- 55 J. X. McDermott, M. E. Wilson and G. M. Whitesides, *J. Am. Chem. Soc.*, 1976, **98**, 6529–6536.
- 56 W. O. Siegl, *J. Org. Chem.*, 1977, **42**, 1872–1878.
- 57 D. Baird, W. Maehlmann, R. Bereman and P. Singh, *J. Coord. Chem.*, 1997, **42**, 107–126.
- 58 T. G. Appleton, J. R. Hall, S. F. Ralph and C. S. Thompson, *Inorg. Chem.*, 1984, **23**, 3521–3525.
- 59 v. B. Origin7.5TM SRO, Origin Lab Corporation, Northampton, One, Northampton, MA, 01060, USA, Editon edn., 2003.
- 60 C. Lee, W. Yang and R. G. Parr, *Phys. Rev. B: Condens. Matter*, 1988, **37**, 785.
- 61 A. D. Becke, *Phys. Rev. A*, 1988, **38**, 3098.
- 62 A. D. Becke, *J. Chem. Phys.*, 1993, **98**, 5648.
- 63 T. Shoeib and B. L. Sharp, *Metallomics*, 2012, **4**, 1308–1320.
- 64 T. Ziegler, *Chem. Rev.*, 1991, **91**, 651–667.
- 65 H.-M. Wen, Y.-H. Wu, Y. Fan, L.-Y. Zhang, C.-N. Chen and Z.-N. Chen, *Inorg. Chem.*, 2010, **49**, 2210–2221.
- 66 N. T. Abdel Ghani and A. M. Mansour, *Eur. J. Med. Chem.*, 2012, **47**, 399–411.
- 67 A. B. Yongye, M. A. Giulianotti, A. Nefzi, R. A. Houghten and K. Martínez-Mayorga, *J. Comput.-Aided Mol. Des.*, 2010, **24**, 225–235.
- 68 B. A. Blight, S.-B. Ko, J. Lu, L. F. Smith and S. Wang, *Dalton Trans.*, 2013, **42**, 10089–10092.
- 69 G. W. Trucks, M. J. Frisch, H. B. Schlegel, G. E. Scuseria, J. R. Cheeseman, M. A. Robb, G. Scalmani, V. Barone, G. A. Petersson, B. Mennucci, H. Nakatsuji, M. Caricato, X. Li, A. F. Izmaylov, H. P. Hratchian, J. Bloino, G. Zheng, M. Hada, J. L. Sonnenberg, M. Ehara, K. Toyota, R. Fukuda, M. Ishida, J. Hasegawa, T. Nakajima, Y. Honda, O. Kitao, T. Vreven, H. Nakai, J. A. Montgomery Jr., J. E. Peralta, M. Bearpark, F. Ogliaro, J. J. Heyd, E. Brothers, K. N. Kudin, R. Kobayashi, V. N. Staroverov, J. Normand, K. Raghavachari, J. C. B. A. Rendell, S. S. Iyengar, J. Tomasi, M. Cossi, J. M. M. N. Rega, M. Klene, J. E. Knox, J. B. Cross, C. Adamo, V. Bakken, J. Jaramillo, R. Gomperts, R. E. Stratmann, O. Yazyev, A. J. Austin, R. Cammi, C. Pomelli, R. L. Martin, J. W. Ochterski, K. Morokuma, V. G. Zakrzewski, G. A. Voth, P. Salvador, J. J. Dannenberg, S. Dapprich, O. Farkas, A. D. Daniels, J. B. Foresman, J. V. Ortiz, J. Cioslowski and D. J. Fox, *Gaussian 09 (Revision A. 1)*, Inc., Wallingford, CT, 2009.
- 70 F. A. Carey and R. J. Sundberg, *Advanced Organic Chemistry*, Plenum, USA, 4th edn, 2001.
- 71 T. H. Lowry and K. S. Richardson, *Mechanism and Theory in Organic Chemistry*, Harper & Row, New York, 3rd edn, 1987.
- 72 F. A. Carey and R. A. Sundberg, *Advanced Organic Chemistry, Part A: Structure and Mechanisms*, Springer, New York, 5th edn, 2007.

- 73 P. Geerlings, F. De Proft and W. Langenaeker, *Chem. Rev.*, 2003, **103**, 1793–1874.
- 74 L. J. Bartolotti and P. W. Ayers, *J. Phys. Chem. A*, 2005, **109**, 1146–1151.
- 75 R. G. Pearson, *J. Chem. Sci.*, 2005, **117**, 369.
- 76 P. K. Chattaraj and B. Maiti, *J. Am. Chem. Soc.*, 2003, **125**, 2705–2710.
- 77 R. Vijayaraj, V. Subramanian and P. Chattaraj, *J. Chem. Theor. Comput.*, 2009, **5**, 2744–2753.
- 78 R. G. Parr and R. G. Pearson, *J. Am. Chem. Soc.*, 1983, **105**, 7512–7516.
- 79 M. G. Evans and M. Polanyi, *Trans. Faraday Soc.*, 1935, **31**, 875–894.
- 80 W. C. Schiessl, N. K. Summa, C. F. Weber, S. Gubo, C. Dücker-Benfer, R. Puchta, N. J. van Eikema Hommes and R. van Eldik, *Z. Anorg. Allg. Chem.*, 2005, **631**, 2812–2819.
- 81 M. T. Ashby, *Comments Inorg. Chem.*, 1990, **10**, 297–313.
- 82 S. G. Murray and F. R. Hartley, *Chem. Rev.*, 1981, **81**, 365–414.
- 83 K. L. Garner, L. F. Parkes, J. D. Piper and J. G. Williams, *Inorg. Chem.*, 2009, **49**, 476–487.
- 84 N. Martín, J. L. Segura and C. Seoane, *J. Mater. Chem.*, 1997, **7**, 1661–1676.
- 85 M. Adachi and Y. Murata, *J. Phys. Chem. A*, 1998, **102**, 841–845.
- 86 M. Adachi and Y. Nagao, *Chem. Mater.*, 2001, **13**, 662–669.
- 87 A. Juris, F. Barigelletti, V. Balzani, P. Belser and A. Von Zelewsky, *Inorg. Chem.*, 1985, **24**, 202–206.
- 88 M. Das and S. E. Livingstone, *J. Chem. Soc., Dalton Trans.*, 1975, 452–455.
- 89 N. Martin, R. Behnisch and M. Hanack, *J. Org. Chem.*, 1989, **54**, 2563–2568.
- 90 T. Suzuki, C. Kabuto, Y. Yamashita, T. Mukai, T. Miyashi and G. Saito, *Bull. Chem. Soc. Jpn.*, 1988, **61**, 483–493.
- 91 J. Brooks, Y. Babayan, S. Lamansky, P. I. Djurovich, I. Tsyba, R. Bau and M. E. Thompson, *Inorg. Chem.*, 2002, **41**, 3055–3066.
- 92 J. D. Atwood, *Inorganic and organometallic reaction mechanisms*, VCH Publishers, 1997.
- 93 R. Van Eldik, T. Asano and W. Le Noble, *Chem. Rev.*, 1989, **89**, 549–688.